

γ	Chemical reaction parameter	ν	Kinematic Viscosity
ϕ	Non-dimensional concentration	ψ	Stream function
θ	Non-dimensional temperature	Ω	Angular Velocity about the y-axis

1. Introduction

The study of rotating flow and heat transfer has received wide interest in modern fluid dynamics research with applications in geophysics and planetary sciences. Anwar Beg et. al. (2005) have studied convection heat transfer in a rotating fluid in a thermally stratified high-porosity medium, they employed numerical finite difference method to solve the boundary layer equations. Chamkha et. al (2006) investigated double diffusive convection of a rotating fluid over a surface embedded in a thermally stratified high-porosity medium. Mbeledogu and Ogulu (2007) analyzed heat and mass transfer of an unsteady MHD natural convection flow of a rotating fluid past a vertical flat plate in the presence of radiative heat transfer. Bhargava et. al. (2008) studied transient couette flow in a rotating non-Darcian porous medium parallel plate configuration: network simulation method solutions. Salah et. al (2011) investigated new exact solutions for MHD transient rotating flow of a second-grade fluid in a porous medium. Chauhan and Agarwal (2012) have been studied effects of hall current on MHD couette flow in a channel partially filled with a porous medium in a rotating system.

Most of the papers treated permeability of the porous medium as constant. Schwartz and Smith (1953) investigated and reported porosity is not constant but varies from the wall to the interior due to variation in permeability. At first Vafai and Tien (1981) studied boundary and inertia effects on flow and heat transfer in a porous media of constant and variable porosity. They have observed that the great influence of the variation of porosity and permeability take place in velocity and heat transfer. Pal and Mondal (2009) considered radiation effects on combined convection over a vertical flat plate embedded in a porous medium of variable porosity. Pal (2010) investigated Magnetohydrodynamic non-Darcy mixed convection heat transfer from a vertical heated plate embedded in a porous medium with variable porosity. Prasad et.al (2012) studied thermal radiation effects on magnetohydrodynamic free convection heat and mass transfer from a sphere in a variable porosity regime.

All the above mentioned studies confined their discussions by assuming constant fluid properties. However, it is well known that the physical properties of fluid may vary significantly with temperature. Seddeek and Salama (2007) have considered the effect of temperature dependent viscosity and thermal conductivity on unsteady MHD convective heat transfer past a semi-infinite vertical porous moving plate with variable suction. Mukhopadhyay (2009) analyzed unsteady boundary layer flow and heat transfer past a porous stretching sheet in presence of variable viscosity and thermal diffusivity. Non-Darcy free convection flow over a horizontal cylinder in a saturated porous medium with variable properties is investigated by Hassanien and Rashed (2011). Vajravelu et.al (2013) studied unsteady convective boundary layer flow of a viscous fluid at a vertical surface with variable fluid properties.

Motivated by the above literature and application, the present study explores the effects of variable porosity, variable thermal conductivity and chemical reaction on mixed convective boundary layer flow, heat and mass transfer over a vertical plate embedded in a porous medium in a rotating system. In the present article we study the influence of the governing physical parameters, variable porosity, variable thermal conductivity and chemical reaction parameter, on heat and mass transfer using a Runge-Kutta method with shooting technique (see Narayana et.al (2013) and Srinivasacharya and Swamy Reddy (2013)). To the best of my knowledge such a study is not appeared in the scientific literature.

2. Mathematical Formulation

Let us consider steady, two-dimensional, laminar, incompressible, combined heat and mass transfer flow from a permeable vertical plate embedded in a variable porosity medium in rotating system. Fig. 1 illustrates the physical model and coordinate system. Here x is measured along the vertical plate, y is measured normal to the surface, respectively. It is assumed that the free stream velocity U_∞ , parallel to the vertical plate is constant. The plate is maintained at uniform temperature T_w and uniform concentration C_w which are higher than T_∞ and C_∞ respectively, Where T_∞ and C_∞ temperature and concentration of the fluid far away from the surface of the plate. Initially the plate is at rest, after that the whole system is allowed to rotate with a constant

angular velocity Ω about the y-axis. In light of the above assumptions and under Boussinesq approximations, the boundary layer equations for mass, momentum, energy and concentration can be written as follows:

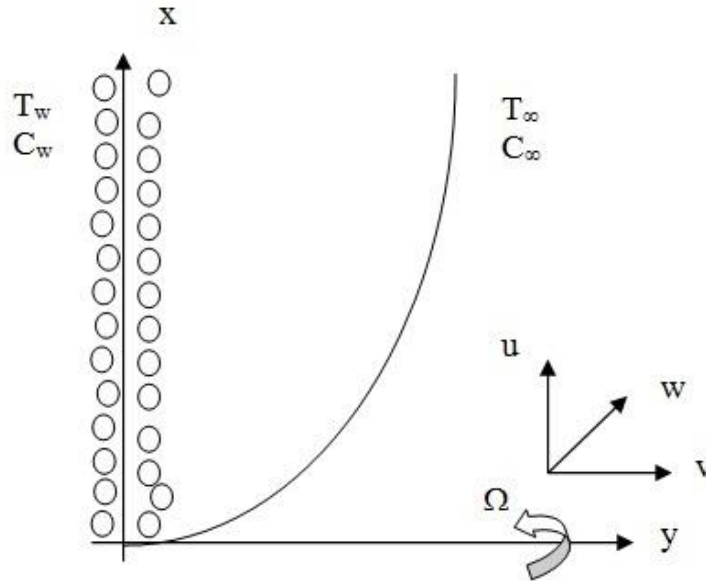


Fig. 1: Physical model and coordinate system

$$\frac{\partial u}{\partial x} + \frac{\partial v}{\partial y} = 0 \tag{1}$$

$$\epsilon^{-2} \left(u \frac{\partial u}{\partial x} + v \frac{\partial u}{\partial y} - 2\Omega w \right) = \epsilon^{-1} \nu \frac{\partial^2 u}{\partial y^2} - \frac{\nu}{K} u + g\beta_t (T - T_\infty) + g\beta_c (C - C_\infty) \tag{2}$$

$$\epsilon^{-2} \left(u \frac{\partial w}{\partial x} + v \frac{\partial w}{\partial y} + 2\Omega u \right) = \epsilon^{-1} \nu \frac{\partial^2 w}{\partial y^2} - \frac{\nu}{K} w \tag{3}$$

$$u \frac{\partial T}{\partial x} + v \frac{\partial T}{\partial y} = \frac{\partial}{\partial y} \left(\alpha \frac{\partial T}{\partial y} \right) + \frac{D_m k_T}{c_s c_p} \frac{\partial^2 C}{\partial y^2} \tag{4}$$

$$u \frac{\partial C}{\partial x} + v \frac{\partial C}{\partial y} = D_m \frac{\partial^2 C}{\partial y^2} + \frac{D_m k_T}{T_m} \frac{\partial^2 T}{\partial y^2} - k_l (C - C_\infty) \tag{5}$$

The boundary conditions are defined as follows:

$$\begin{aligned} u = 0, \quad v = \pm v(x), \quad T = T_w, \quad C = C_w \quad \text{at} \quad y = 0 \\ u \rightarrow U_\infty, \quad T \rightarrow T_\infty, \quad C \rightarrow C_\infty \quad \text{as} \quad y \rightarrow \infty \end{aligned} \tag{6}$$

Where u, v and w denotes velocity components in x, y and z directions, respectively, K is the permeability of the porous medium, ν is the kinematic viscosity, ϵ is the porosity, β_t and β_c are the coefficients of thermal expansion and concentration expansions, respectively, Ω is the angular velocity about the y-axis, T and C are temperature and concentration respectively. α and D_m are thermal and mass diffusivities respectively, k_T is the thermal diffusion ratio, c_p is the specific heat at constant pressure, c_s is the concentration susceptibility, T_m is the mean fluid temperature and k_l is the chemical reaction rate and g is the acceleration due to gravity.

The fluid properties are assumed to be isotropic and constant, except for the fluid thermal conductivity α . We assume that the fluid thermal conductivity is to be varying as a linear function of the temperature in the form (Seddeek and Salem (2007)):

$$\alpha = \alpha_o (1 + E(T - T_\infty))$$

Where E is a constant depending on the nature of the fluid and α_o is the thermal diffusivity at the surface temperature T_w . In non-dimensional form

$$\alpha = \alpha_o(1 + \beta\theta) \tag{7}$$

where $\beta = E(T_w - T_\infty)$ is the thermal conductivity parameter. The range of the β can be taken as $-0.1 \leq \beta \leq 0$ for lubrication oils, $0 \leq \beta \leq 0.12$ for water.

Using Eq. (7), Eq. (4) becomes

$$u \frac{\partial T}{\partial x} + v \frac{\partial T}{\partial y} = \alpha_o \frac{\partial}{\partial y} \left((1 + \beta\theta) \frac{\partial T}{\partial y} \right) + \frac{D_m k_T}{c_s c_p} \frac{\partial^2 C}{\partial y^2} \tag{8}$$

We now introduce the following similarity variables

$$\eta = y \sqrt{\frac{U_\infty}{\nu x}}; \quad \psi = \sqrt{\nu x U_\infty} f(\eta); \quad \theta(\eta) = \frac{T - T_\infty}{T_w - T_\infty}; \quad \phi(\eta) = \frac{C - C_\infty}{C_w - C_\infty}; \quad g = \frac{w}{U_\infty} \tag{9}$$

where ψ is the stream function such that $(u, v) = \left(\frac{\partial \psi}{\partial y}, -\frac{\partial \psi}{\partial x} \right)$ and η is the similarity variable.

Using Eq. (9), Eqs. (1)-(3), (5) and (8) become

$$\varepsilon^{-1} f''' + \varepsilon^{-2} \left(\frac{1}{2} f f'' + Rg \right) + g_s \theta + g_c \phi - Kf' = 0 \tag{10}$$

$$\varepsilon^{-1} g'' + \varepsilon^{-2} \left(\frac{1}{2} f g' - Rf' \right) - Kg = 0 \tag{11}$$

$$(1 + \beta\theta)\theta'' + \beta(\theta')^2 + \frac{1}{2} \text{Pr} f\theta' + \text{Pr} Du \phi'' = 0 \tag{12}$$

$$\phi'' + \frac{1}{2} Sc f \phi' - Sc \gamma \phi + Sc Sr \theta'' = 0 \tag{13}$$

The associated boundary conditions are

$$f = f_w, \quad f' = 0, \quad g = 0, \quad \theta = 1, \quad \phi = 1 \quad \text{at} \quad \eta \rightarrow 0 \tag{14}$$

$$f' \rightarrow 1, \quad g \rightarrow 0, \quad \theta \rightarrow 0, \quad \phi \rightarrow 0 \quad \text{as} \quad \eta \rightarrow \infty$$

where $R = \frac{4\Omega x}{U_\infty}$ is the rotational parameter, $g_s = \frac{Gr}{\text{Re}^2}$ is the temperature buoyancy parameter,

$g_c = \frac{Gm}{\text{Re}^2}$ is the mass buoyancy parameter, $Gr = \frac{g\beta_l(T_w - T_\infty)x^3}{\nu^2}$ is the Grashof number,

$Gm = \frac{g\beta_c(C_w - C_\infty)x^3}{\nu^2}$ is the modified Grashof number, $K = \frac{2\nu x}{kU_\infty}$ is the Darcy number, $\text{Pr} = \frac{\nu}{\alpha_o}$ is the

Prandtl number, $Sc = \frac{\nu}{D}$ is the Schmidt number, $Du = \frac{D_m k_T}{c_s c_p} \frac{(C_w - C_\infty)}{(T_w - T_\infty)}$ is the Dufour parameter,

$Sr = \frac{D_m k_T}{\nu T_m} \frac{(T_w - T_\infty)}{(C_w - C_\infty)}$ is the Soret number, $\gamma = \frac{k_l(C_w - C_\infty)2x}{U_\infty}$ is the chemical reaction parameter and

$f_w = \frac{2xv(x)}{\nu} \text{Re}^{-1/2}$ is the dimensionless suction velocity.

3. Numerical Method of Solution

The a set of nonlinear non-homogeneous differential equation (10)-(13) with corresponding boundary conditions (14) are solved numerically using a shooting technique along with fourth order Runge-Kutta integration. In this method, Equations (10)-(13) are converted into the following system of linear differential equations of first order

$$\begin{aligned}
 f' &= L, \quad f'' = M, \quad g' = N, \\
 \theta' &= P, \quad \phi' = Q \\
 f''' &= -\varepsilon \left(\varepsilon^{-2} \left(\frac{1}{2} fM + R g \right) - K L + g_s \theta + g_c \phi \right) \\
 g'' &= -\varepsilon \left(\varepsilon^{-2} \left(\frac{1}{2} fN - R L \right) - K g \right) \\
 \theta'' &= \frac{-1}{(1 + \beta \theta) - \text{Pr} Du Sc Sr} \left[\beta (P)^2 + \frac{1}{2} \text{Pr} f (P - Du Sc Q) + \text{Pr} Du Sc \gamma \phi \right] \\
 \phi'' &= \frac{-1}{\text{Pr} Sc Sr Du - (1 + \beta \theta)} \left[Sc Sr \beta (P)^2 + \frac{1}{2} Sc f (Sr Pr P - (1 + \beta \theta) Q) \right. \\
 &\quad \left. + (1 + \beta \theta) Sc \gamma \phi \right]
 \end{aligned} \tag{15}$$

The boundary conditions are

$$\begin{aligned}
 f(0) &= f_w, \quad L(0) = 0, \quad g(0) = 0, \quad \theta(0) = 1, \quad \phi(0) = 1 \\
 L(\infty) &= 1, \quad g(\infty) = 0, \quad \theta(\infty) = 0, \quad \phi(\infty) = 0
 \end{aligned} \tag{16}$$

As the initial values for $L(0) = f''(0)$, $N(0) = g'(0)$, $P(0) = \theta'(0)$ and $Q(0) = \phi'(0)$ are not specified in the boundary conditions, assume some suitable values for $M(0)$, $N(0)$, $P(0)$ and $Q(0)$. Then Eqs. (15) are integrated using the fourth order Runge-Kutta method from $\eta = 0$ to $\eta = \eta_{\max}$ over successive step lengths 0.01. Here, η_{\max} is the value of η at ∞ and chosen large enough so that the solution shows little further change for η larger than η_{\max} . The accuracy of the assumed values for $M(0)$, $N(0)$, $P(0)$ and $Q(0)$ are then checked by comparing the calculated values of L , g , θ and ϕ at $\eta = \eta_{\max}$ with their given value at $\eta = \eta_{\max}$. If a difference exists, another set of initial values for $M(0)$, $N(0)$, $P(0)$ and $Q(0)$ are assumed and the process is repeated. This process is continued until the agreement between the calculated and the given condition at $\eta = \eta_{\max}$ is within the specified degree of accuracy 10^{-5} .

4. Local Skin Friction Coefficient, Surface Temperature and Concentration Distribution

The skin friction coefficients are denoted by

$$\begin{aligned}
 \tau_x &= \mu \left(\frac{\partial u}{\partial y} \right)_{y=0} \quad \text{and} \quad \tau_z = \mu \left(\frac{\partial w}{\partial y} \right)_{y=0} \quad \text{which are proportional to} \\
 &\left(\frac{\partial^2 f}{\partial \eta^2} \right)_{\eta=0} \quad \text{and} \quad \left(\frac{\partial g}{\partial \eta} \right)_{\eta=0}.
 \end{aligned} \tag{17}$$

The Nusselt number and Sherwood number are denoted by

$$\begin{aligned}
 Nu &= -\frac{1}{\Delta T} \left(\frac{\partial T}{\partial y} \right)_{y=0} \quad \text{and} \quad Sh = -\frac{1}{\Delta C} \left(\frac{\partial C}{\partial y} \right)_{y=0} \\
 \text{In non-dimensional form} \\
 Nu &= \left(\frac{\partial \theta}{\partial \eta} \right)_{\eta=0} \quad \text{and} \quad Sh = \left(\frac{\partial \phi}{\partial \eta} \right)_{\eta=0}.
 \end{aligned} \tag{18}$$

5. Comparison with Previous Work and Program Validation

To validate the numerical method we compare the results with previously published work by Alam and Rahman (2006) these results are reported in Table 1. A comparison of the surface temperature and local skin friction

coefficient obtained in the present work with $x^{\frac{1}{5}} = \xi$, $M=0$ and $\gamma=0$ and obtained by Merkin and Pop (1996) and Pozzi and Lupo (1988) have been shown in Table 1 and Table 2, respectively. It is clearly seen that there is an excellent agreement among the respective results.

Table 1: Numerical values of Nusselt number and Sherwood number are compared with those of Alam and Rahman (2006) by taking $\varepsilon = 0$, $\beta = 0$, $\gamma = 0$, $R = 0$.

Parameters		Alam and Rahman (2006)		Present Results	
Du	Sr	Nu	Sh	Nu	Sh
0.030	2.0	0.5310	0.1292	0.5309	0.1288
0.037	1.6	0.5299	0.1605	0.5301	0.1602
0.050	1.2	0.5285	0.1921	0.5289	0.1920
0.060	1.0	0.5275	0.2077	0.5270	0.2075
0.075	0.8	0.5263	0.2233	0.5258	0.2230
0.120	0.5	0.5230	0.2470	0.5225	0.2465
0.600	0.1	0.4908	0.2817	0.4905	0.2812

6. Results and Discussion

In this study, the efficient method Runge-Kutta method with shooting technique has been used to solve the governing equations (10)-(13) subject to the boundary conditions (14). Selected computations have been found to study the influence of variable porosity regime, variable thermal conductivity and chemical reaction parameter on primary and secondary velocity, skin friction components, Nusselt number and Sherwood numbers. In all cases we have assumed the default values (unless, otherwise specified) for the parameters: $\varepsilon=2$, $R=0.2$, $g_s=1$, $g_c=0.1$, $K=0.05$, $Pr=0.71$, $\beta=0.5$, $Sc=0.22$, $\gamma=0.5$, $fw=0.5$.

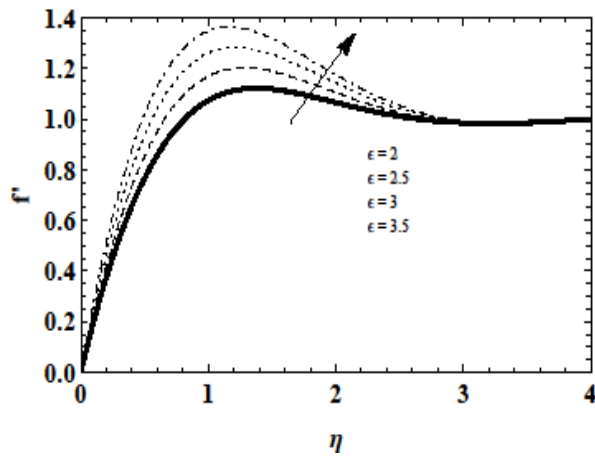


Fig. 2: Velocity profile for various values of variable porosity regime.

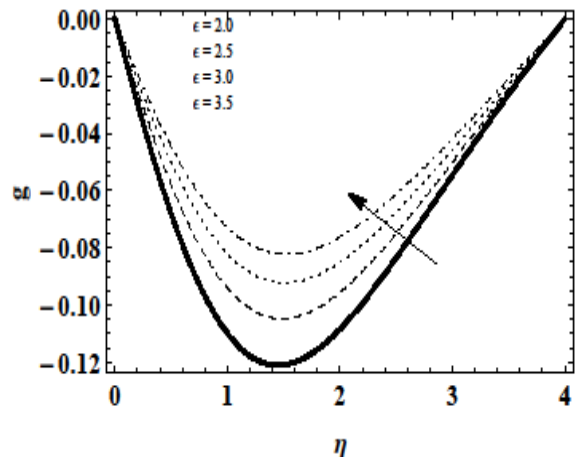


Fig. 3: Secondary Velocity profile for various values of variable porosity regime

Figs. (2) – (5) depicts the influence of porosity (ε) on the boundary layer variables, primary and secondary velocity profiles, temperature profile and concentration profiles. Increasing porosity results an enhancement in primary and secondary velocity profile but retards in temperature and concentration profiles, i.e. the boundary layer is cooled.

Figs. (6) – (9) illustrates the influence of variable thermal conductivity (β) on the boundary layer variables, f' , g , θ , ϕ . From Fig. (6) We observed that primary velocity increases with increase in β . i.e., increase the velocity boundary layer thickness. In Fig. (7) a similar response for the secondary velocity field is observed, as with the primary velocity profiles. Secondary velocity values are continuously decreased with increasing

porosity. An increase in β , causes an increment in temperature profile with distance into the boundary layer, i.e., accelerate the thermal boundary layer but the concentration profile decreases with increase in β .

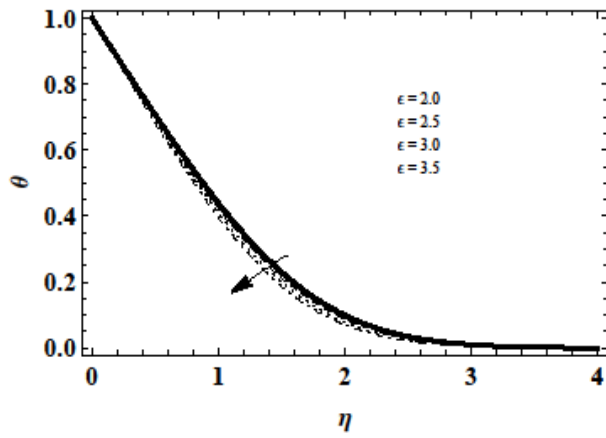


Fig. 4: Temperature profile for various values of variable porosity regime.

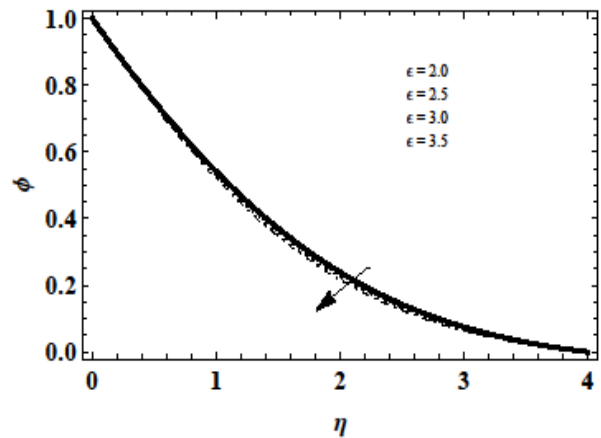


Fig. 5: Concentration profile for various values of variable porosity regime.

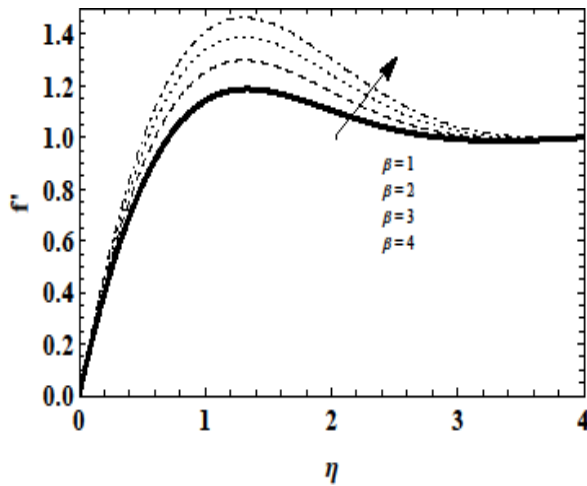


Fig. 6: Velocity profile for various values of variable thermal conductivity.

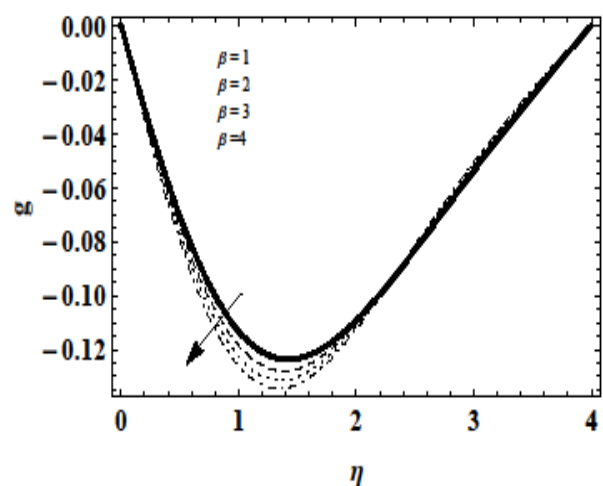


Fig. 7: Secondary velocity profile for various values of variable thermal conductivity

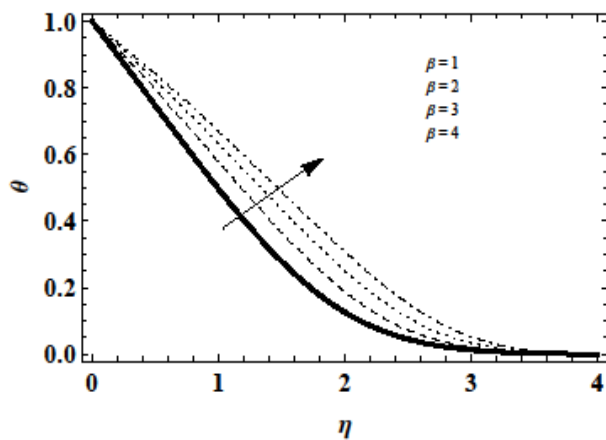


Fig. 8: Temperature profile for various values of variable thermal conductivity.

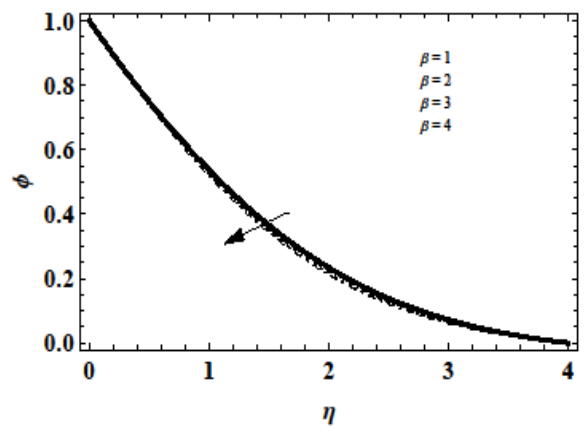


Fig. 9: Concentration profile for various values of variable thermal conductivity.

Figs. (10) – (11) shows the influence of chemical reaction parameter on primary velocity and concentration profiles. With a dramatic increase in chemical reaction parameter (γ) there is a very slight deceleration in primary velocity in the boundary layer regime as shown in Fig. (10). The deceleration in the flow results in thinner velocity boundary layer. It shows that concentration distribution decrease when the chemical reaction parameter is increased and it causes the thinner concentration boundary layer. An increase in concentration of the diffusing species increase the mass diffusion and thus the fluid velocity and temperature increase.

The non-dimensional skin-friction components τ_x , and τ_z , Nusselt number (Nu) and Sherwood number (Sh) are reported in Tables 2-3 for different values of variable porosity regime (ϵ), variable thermal conductivity (β) and chemical reaction parameter (γ). From Table 2 we observed that increasing ϵ tends to accelerate skin friction components τ_x , τ_z , Nusselt number and Sherwood number. Increasing ϵ clearly serves to reduce presence of matrix fibers in the boundary layer regime which therefore gives rise to a lower resistance to the fluid flow and shear faster past the vertical surface. From Table 3 we say that skin friction component τ_x , and Sherwood number increases while skin friction component τ_z and Nusselt number decreases with increase in variable thermal conductivity parameter (β) and $\beta=0$ gives the result in case of uniform thermal conductivity. It is obvious that increasing chemical reaction serves to enhance the rate of interfacial mass transfer and hence rate of mass transfer is more pronounced. Thus, from Table 3 it is clear that skin friction component τ_x , and Nusselt number decreases while skin friction component τ_z and Sherwood number increases with the increase of chemical reaction parameter.

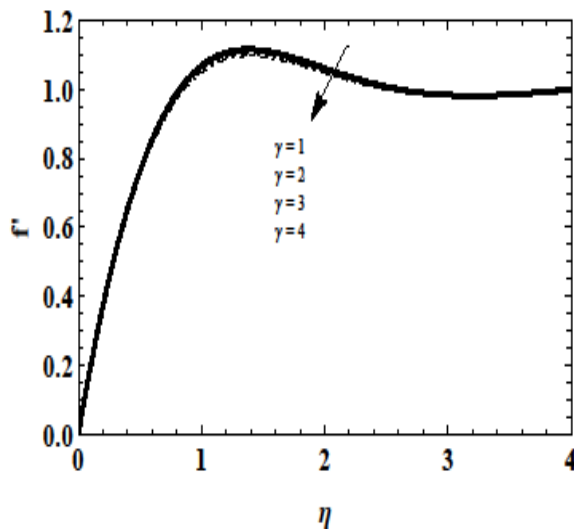


Fig. 10: Velocity profile for various values of chemical reaction parameter.

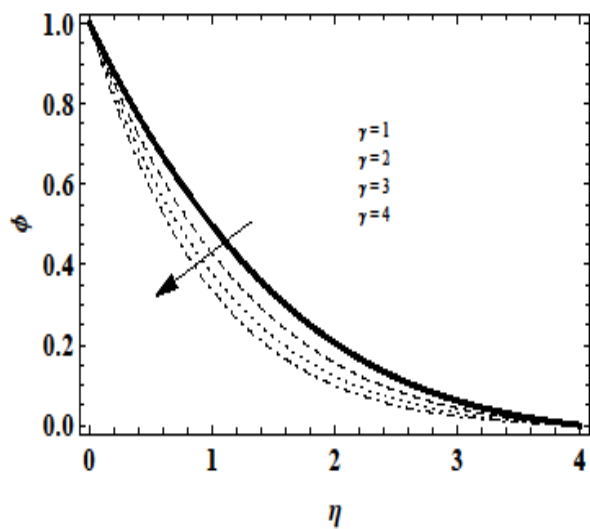


Fig. 11: Concentration profile for various values of chemical reaction parameter.

Table 2: Numerical values of Skin friction components, Nusselt number and Sherwood number for different values of variable porosity regime.

ϵ	τ_x	τ_z	Nu	Sh
1.0	1.6895	-0.2698	0.5649	0.524
1.5	1.8699	-0.1928	0.5787	0.531
2.0	2.1375	-0.1530	0.5954	0.538
2.5	2.4172	-0.1282	0.6120	0.546

Table 3: Numerical values of skin friction components, Nusselt number and Sherwood number for different values of variable thermal conductivity and chemical reaction parameter

β	γ	τ_x	τ_z	Nu	Sh
1.0	0.5	2.2454	-0.1586	0.4977	0.5435
1.2	0.5	2.2826	-0.1606	0.4703	0.5454
1.4	0.5	2.3171	-0.1624	0.4470	0.5471
1.6	0.5	2.3494	-0.1642	0.4271	0.5487
0.5	1.0	2.12901	-0.1525	0.5945	0.6293
0.5	1.5	2.1220	-0.1521	0.5938	0.7106
0.5	2.0	2.1159	-0.1517	0.5932	0.7847

7. Conclusion

From above mentioned studies, following conclusion can be drawn:

- Primary and secondary velocity profiles increases while decrease in temperature and concentration profiles with increase in variable porosity (ϵ).
- An increase in variable thermal conductivity cause to increase in primary velocity and temperature profiles while decrease in secondary velocity and concentration profiles.
- Increase in chemical reaction parameter tends to decrease in primary velocity while increase in concentration profile.
- Increasing variable porosity results an enhancement in skin friction components, Nusselt number and Sherwood number.
- Increasing variable thermal conductivity has been shown to elevate skin friction component τ_x and Sherwood number but depress skin friction component τ_z and Sherwood number.
- Increasing chemical reaction parameter have been found to decelerate skin friction component τ_x and Nusselt number and accelerate skin friction component τ_z and Sherwood number.

Acknowledgement

The authors would like to thank to the Department of Science and Technology, New Delhi, India for providing financial support to enable conducting this research work under Inspire Program.

References

- Alam, M.S. and Rahman, M.M. (2006): Dufour and Soret effects on mixed convection flow past a vertical porous flat plate with variable suction. *Nonlinear Analysis: Modelling and Control*, Vol. 11, No.1, pp. 3-12.
- Al-Humoud, J.M. and Chamkha, A.J. (2006): Double diffusive convection of a rotating fluid over a surface embedded in a thermally stratified high-porosity medium. *Heat and Technology*, Vol. 24 No. 1 pp. 51-59.
- Anwar Beg, O. Takhar, H.S. Beg, T.A. Chamkha, A.J. Nath, G. and Majeed, R. (2005): Modelling convection heat transfer in a rotating fluid in a thermally stratified high-porosity medium: Numerical finite difference solutions. *International Journal of Fluid Mechanics Research*, Vol. 32 No. 4 pp. 383-401. <http://dx.doi.org/10.1615/InterJFluidMechRes.v32.i4.10>
- Anwar Beg, O. Takhar, H.S. Zueco, J. Sajid, A. and Bhargava, R (2008): Transient couetto flow in a rotating non-Darcian porous medium parallel plate configuration: network simulation method solutions. *Acta Meccanica*, Vol. 200 pp. 129-144. <http://dx.doi.org/10.1007/s00707-008-0040-8>
- Chauhan, D.S. and Agarwal, R. (2012): Effects of hall current on MHD couette flow in a channel partially filled with a porous medium in a rotating system. *Meccanica*, Vol. 47, pp. 405-421.
- Hassanien, I.A. and Rashed, Z.Z. (2011): Non-Darcy free convection flow over a horizontal cylinder in a saturated porous medium with variable viscosity, thermal conductivity and mass diffusivity. *Communications in*

Nonlinear Science and Numerical Simulations, Vol. 16 pp. 1931-1941. <http://dx.doi.org/10.1016/j.cnsns.2010.08.030>

Mbeledogu, I.U. and Ogulu, A. (2007): Heat and mass transfer of an unsteady MHD natural convection flow of a rotating fluid past a vertical flat plate in the presence of radiative heat transfer. *International Journal of Heat and Mass Transfer*, Vol. 50 pp. 1902-1908. <http://dx.doi.org/10.1016/j.ijheatmasstransfer.2006.10.016>

Mukhopadhyay, S. (2009): Unsteady boundary layer flow and heat transfer past a porous stretching sheet in presence of variable viscosity and thermal diffusivity. *International Journal of Heat and Mass Transfer*, Vol. 52, pp. 5213-5217. <http://dx.doi.org/10.1016/j.ijheatmasstransfer.2009.04.013>

Narayana, M. Khidir, A.A. Sibanda, P. and Murthy, P.V.S.N. (2013): Viscous dissipation and thermal radiation effects on mixed convection from a vertical plate in a Non-Darcy porous medium. *Transport in Porous Media*, Vol.96, pp.419-428. <http://dx.doi.org/10.1007/s11242-012-0096-8>

Pal, D. and Mondal, H. (2009): Radiation effects on combined convection over a vertical flat plate embedded in a porous medium of variable porosity. *Acta Meccanica*, Vol. 44, pp. 133-144.

Pal, D. (2010): Magnetohydrodynamic non-Darcy mixed convection heat transfer from a vertical heated plate embedded in a porous medium with variable porosity. *Communication in Nonlinear Science and Numerical Simulation*, Vol. 15, pp. 3974-3987. <http://dx.doi.org/10.1016/j.cnsns.2010.02.003>

Prasad, V.R. Vasu, B. Anwar Beg, O. and Parshad, R.D. (2012): Thermal radiation effects on magnetohydrodynamic free convection heat and mass transfer from a sphere in a variable porosity regime. *Communication in Nonlinear Science and Numerical Simulation*, Vol. 17 pp. 654-671. <http://dx.doi.org/10.1016/j.cnsns.2011.04.033>

Salah, F. Aziz, Z.A. and Ching, D.L.C. (2011): New exact solutions for MHD transient rotating flow of a second-grade fluid in a porous medium. *Journal of Applied Mathematics*, pp. 1-8.

Schwartz, C.E. and Smith, J. M. (1953). Flow distribution in packed beds. *Ind Eng Chem*, Vol. 45, pp. 1209-1218.

Seddeek, M.A. and Salama, F.A. (2007): The effects of temperature dependent viscosity and thermal conductivity on unsteady MHD convective heat transfer past a semi-infinite vertical porous moving plate with variable suction. *Computational Material Science*, Vol. 40 pp. 186-192. <http://dx.doi.org/10.1016/j.commatsci.2006.11.012>.

Srinivasacharya, D. and Swamy Reddy, G. (2013): Mixed convection heat and mass transfer over a vertical plate in a power-law fluid-saturated porous medium with radiation and chemical reaction effects. *Heat Transfer-Asian Research*, Vol.42(6), pp. 485-499. <http://dx.doi.org/10.1002/htj.21058>

Vafai, K. and Tien, C.L. (1981): Boundary and inertia effects on flow and heat transfer in porous media. *International Journal of Heat and Mass Transfer*, Vol. 24, pp. 195-203. [http://dx.doi.org/10.1016/0017-9310\(81\)90027-2](http://dx.doi.org/10.1016/0017-9310(81)90027-2)

Vajravelu, K. Prasad, K.V. and Chiu-on, Ng. (2013): Unsteady convective boundary layer flow of a viscous fluid at a vertical surface with variable fluid properties. *Nonlinear Analysis: Real World Application*, Vol. 14, pp. 455-464. <http://dx.doi.org/10.1016/j.nonrwa.2012.07.008>